

NATURAL CONVECTION IN TRIANGULAR ENCLOSURES

C.R. Maliska, S. Polina and A.F.C. Silva
Universidade Federal de Santa Catarina
P.O. Box, 476 - Florianópolis - SC
Brazil

ABSTRACT

The natural convection heat transfer in triangular enclosures is analyzed numerically with the main goal of comparing the numerical results with the experimental ones available in the literature. As a second objective the paper reports the equivalent conductivity for the triangular cavity with different height/base relations and for Rayleigh number ranging from 0 to $5.3 \cdot 10^6$. The numerical results are obtained using a finite volume method in boundary-fitted coordinates. The equivalent conductivity calculated numerically agrees very well with the experimental ones.

INTRODUCTION

Natural convection heat transfer is a subject which has received enormous attention with the advent of the numerical techniques. In the engineering point of view there are many situations where it is necessary to know the heat transfer coefficient inside enclosures for better designing engineering equipments. If a review is carried out trying to measure the amount of publications dealing with the numerical solution of the natural convection problem inside rectangular and square cavities, one is going to conclude that almost everything related to these cavities were already investigated. Boundary conditions ranging from the usual two vertical heated walls to mixed boundary conditions in one wall are reported in the specialized literature. The preference for this geometry is due to the

easiness in designing computer codes for the numerical solution of the governing partial differential equations.

Triangular enclosures, in the other hand, has received very little attention, despite its important applications, specially in the simulation of a roof in the calculation of thermal behaviour of buildings. Among the available work in the literature, FLACK et alii (1979) conducted an experimental work where the bottom side of the triangular enclosure is insulated while the left side is heated and the right one cooled. FLACK (1980), also measured the heat transfer coefficients in a triangular cavity where the bottom side is heated or cooled, instead of insulated.

A recent work by POULIKAKOS and BEJAN (1983) reports a comprehensive study of the natural convection flow inside a triangular cavity with a warm bottom wall where an asymptotic analysis, including transient response is also reported.

In this paper it is analyzed the situation studied by FLACK (1979) with the main goal of comparing the numerical and experimental results, in a continuation process of assessing the numerical method used in this work. The paper also analyses the problem for angles between the inclined walls of 60, 90 and 120 degrees.

PROBLEM FORMULATION AND NUMERICAL METHODOLOGY

The problem under analysis is the natural convection inside a triangular enclosure as shown in Fig. 1, where the appropriate boundary conditions are indicated. Using the Boussinesq approximation, the governing differential equations, written in the ξ - η generalized coordinate system are, for a general ϕ variable

$$\frac{\rho}{J} \frac{\partial \phi}{\partial \xi} + \rho \frac{\partial}{\partial \xi} (U\phi) + \rho \frac{\partial}{\partial \eta} (V\phi) + \bar{P}\phi = \quad (1)$$

$$\frac{\partial}{\partial \xi} (C_1 \frac{\partial \phi}{\partial \xi} + C_2 \frac{\partial \phi}{\partial \eta}) + \frac{\partial}{\partial \eta} (C_1 \frac{\partial \phi}{\partial \xi} + C_2 \frac{\partial \phi}{\partial \eta}) + \bar{S}\phi$$

where the parameters for each equation are given in Table I. The other variables appearing in Eq. (1) are given by

$$\begin{aligned}
 U &= y_{\eta} u - x_{\eta} v & V &= x_{\xi} v - y_{\xi} u & J &= (x_{\xi} y_{\eta} - x_{\eta} y_{\xi})^{-1} \\
 C_1 &= \Gamma^{\phi} J \alpha & C_2 &= -\Gamma^{\phi} J \beta & C_3 &= \Gamma^{\phi} J \gamma & (2) \\
 \alpha &= x_{\eta}^2 + y_{\eta}^2 & \beta &= x_{\xi} x_{\eta} + y_{\xi} y_{\eta} & \gamma &= x_{\xi}^2 + y_{\xi}^2
 \end{aligned}$$

Details of the numerical model can be found in MALISKA (1984) and only the major features will be reported here. The method solves the conservation equation in a general curvilinear coordinate system (ξ, η) whose coordinate lines are coincident with the boundary of the domain. The equations are solved in a segregated manner and an extra-equation for pressure is constructed using the PRIME method, as described in MALISKA (1981). In this method the momentum equations are solved in a point iteration fashion performing one sweep in the domain for each coefficient updating. The linear system of equation for pressure and temperature are solved using the nine point version of the MSI - Modified Strongly Implicit procedure of SCHNEIDER and ZEDAN (1981).

BRIEF DESCRIPTION OF FLACK'S EXPERIMENT

The air filled cavity consist of two constant temperature water tanks with inclined bottoms and an horizontal adiabatic wall, as shown in Fig. 2. The inclined plates are 10.78 cm long (L) and 25.4 cm wide and are made of polished aluminum 1.27 cm thick. The temperature was measured in each tank bottom (the inclined faces of the triangular enclosure) using six thermocouples. The thermocouples distribution can be seen in the original publication. One tank was maintained at a constant hot temperature by an electric heater and the temperature of the cold surface was kept constant using an ice bath mixture in the second tank. To keep the temperature uniform within 0.5°C both baths were mixed by electrical stirrers.

The bottom surface (the insulated one) was made of bakelite and heavily insulated.

A Wollaston prism schlieren interferometer was used to make the heat transfer measurements. The local temperature gradients are

proportional to the fringe shift. Proper equations for this calculation is found in FLACK et alii (1979) where they also report that heat transfer measurements around a isothermal flat plate were obtained with 5 percent difference when compared with previous correlations. This was done for checking the apparatus.

NUMERICAL EXPERIMENTS

When attempting to obtain a numerical solution of a problem the grid resolution study must be carried out in order to get the grid independent solution. In this particular problem if the analytical solution is obtained for the pure conduction problem, one can show that the heat flux at the touching point of the heat and cold walls blows up (ARPACI (1966) and POULIKAKOS and BEJAN (1983)). This is easy to understand since the conduction resistance tends to zero while the temperature gradients is constant, when one moves towards the tip. This poses a difficulty for the numerical solution because there is no grid independent solution for this case since, as the grid is refined, the numerical solution tends to reproduce the analytical results. In this case, the heat calculated numerically at the tip will be larger and larger, influencing the average heat transfer coefficient at the walls considerably. In conclusion, keeping this singularity in the boundary conditions there is no way to obtain a grid independent solution for the problem.

To avoid this numerical problem POULIKAKOS and BEJAN (1983) simply neglected the heat flux along 10 percent of the walls from the tip. One understands that this is not the proper way to by-pass the problem because the heat flux neglected influences considerably the average heat flux. In this paper an average temperature is assumed for the tip and a linear temperature profile is adopted, as sketched in Fig. 5. This strategy removes the singularity at the tip and simulates more realistically the experiment.

PHYSICAL PROPERTIES, GEOMETRIC AND FLOW PARAMETERS

The conservation equations are written in a non dimensionless form and the physical properties, to obtain the Rayleigh and Prandtl numbers, are calculated using an average temperature of 300K. The values of the properties employed for the numerical experiments are

$K=0.0263 \text{ W/mK}$; $\mu=1.846E-05 \text{ kg/ms}$; $C_p=1007 \text{ W/kg } ^\circ\text{C}$ e $Pr=0.707$

and they correspond to a temperature of 300 K.

The Grashof number is evaluated according to

$$Gr = g\beta\cos\gamma(T_H - T_C)L^3/\nu_m^2 \quad (3)$$

with

$$\beta = \frac{2}{(T_H + T_C)} \quad (4)$$

The heat transfer coefficient will be reported using the equivalent conductivity parameter defined as

$$Keq = \frac{\bar{q}}{\bar{q}_{cond}} \quad (5)$$

where \bar{q} is the average heat flux and \bar{q}_{cond} is the average heat flux for $Rs=0$.

The Nusselt number to be compared with the experimental one is defined as

$$\bar{Nu} = \frac{\bar{h}L}{K_m} \quad (6)$$

defining the heat transfer coefficient as

$$\bar{h} = \frac{\bar{q}}{T_H - T_C} \quad (7)$$

and using

$$\bar{q} = -K_m \frac{\partial T}{\partial n} \quad (8)$$

one gets

$$\bar{Nu} = - \frac{\partial T}{\partial n} \frac{L}{T_H - T_C} \quad (9)$$

To conclude the presentation of the relevant parameters Table II brings the geometric relations used for the experimental measurements and the numerical calculations.

NUMERICAL RESULTS

The triangular domain was discretized using boundary-fitted coordinates as shown in Fig. 3, where 24 x 24 finite volumes are used. This grid size was established after carrying out a grid resolution study. It is important to observe the high nonorthogonal region of the grid near the middle of the insulated wall.

To start the comparisons, Fig. 4 shows the local heat flux along the hot and cold walls, including FLACK'S results. It is to be noted that the origin of the axis for the cold and hot wall are different, according to Fig. 2.

Inspecting Fig. 4, drawing attention to the cold wall, one sees that the experimental heat flux shows its maximum of about 330 W/m^2 near $x^*/L=0$, decreasing continuously to zero, while the numerical results show its maximum of about 500 W/m^2 at $x^*/L=0.12$, then decreasing continuously to zero, exhibiting the same behaviour as the experimental results.

Inspecting now the curve for the hot wall one realizes again that the numerical heat flux does not show its maximum at $x^*/L=0$, as does the experimental one. In the numerical case the maximum occurs at $x^*/L=0.07$. The physical situation which occurs at the left corner of the triangular cavity is similar to that at the left bottom corner of a square cavity. For the latter case the maximum Nusselt number is located at about 10 percent from the left corner, according to VAHL DAVIS and JONES (1983). The findings for the triangular cavity are the same, as expected.

Continuing to discuss the results, it's important to present the linear profiles adopted in the top corner of the cavity for avoiding the blow up of the heat flux at that position. Since the hot wall was

assumed to be at 49°C and the cold wall at 19°C, the point at the corner was taken to be at 25°C. Then, a linear profile was assumed for the next 5 elements along the hot and cold wall, as shown in Fig. 5.

Still paying attention to Fig. 4, one can see that the measured heat flux at the top corner is practically the same for the hot and cold wall. For the numerical results this does not happen, being the heat flux near the corner, at the cold wall, 2.8 times greater than at the hot wall. Numerically this relation can not be unity, due to the imposed temperature profile at the walls. Of course, to impose a temperature profile along a portion of the walls (7 percent in this case) is not the appropriate way to treat this boundary condition. It is better than to keep a singular point, but the proper way is to solve the conjugate conduction/convection problem, involving the walls and the fluid.

To conclude the analysis of Fig. 4 the comparison between the average heat flux at the walls is carried out. Using the measured total heat transferred at the walls, and the area of walls, one finds $\bar{q}_h = 140.2 \text{ W/m}^2$ and $\bar{q}_c = 145.7 \text{ W/m}^2$. In the numerical case the average heat flux at the cold and hot walls are exactly the same, due to the conservation principles implied in the algebraic equations, and equal to $\bar{q} = 151.2 \text{ W/m}^2$.

As a global conclusion one could say that the local heat fluxes exhibit the same trends with higher maximum for the numerical results. The average heat flux, by its turn, is in very good agreement with the experimental measurements.

To continue the comparisons Table III shows the average Nusselt number calculated according to Eq.(9) with the experimental values taken from Fig. 9 of FLACK et alii(1979). As can be extracted from the table for $\theta=90$ and 120 the results are in good agreement, showing a maximum difference of 4.1 percent. For $\theta=60$ one has only one result to compare and the agreement is not good, showing a difference of 16.7 percent. Up till now no reason for this difference has been detected.

In Fig. 6 it is shown the equivalent conductivity as defined by Eq.(5), for $\theta=60, 90$ and 120, as a function of the Rayleigh number. As can be seen the heat is transferred by pure conduction up to $Ra=10^3$. This figure depicts an increasing equivalent conductivity for an increasing θ . This means that the natural recirculating flow caused by the buoyance force is more effective for larger angles than for smaller ones. In fact, for $\theta=60$ the heat transferred by conduction is

about 4 times greater than for $\theta=120$ and so, the recirculating flow is less important, relatively to pure conduction, for $\theta=60$ than for $\theta=120$. This does not mean, however, that the heat transfer characteristics for larger are better than for smaller ones. In fact, if the heat transfer characteristics are put in terms of the Nusselt number, as defined in Eq.(9), for a constant Rayleigh number, the Nusselt number decreases with increasing θ . As the Rayleigh number increases, for the three angles studied, the influence of the geometry decreases, since the strong recirculating flow plays a more important role in the heat transfer than the geometry does. The Nusselt number is not shown here, but it can be easily obtained with the help of Fig. 6 and Table III.

To illustrate a bit more the phenomenon, Figs. 7 and 8 depict the temperature and the velocity profiles along the vertical line passing through the top corner, while Fig. 9 shows the velocity vector plot for $\theta=90$ and $Ra=3.96 \cdot 10^6$.

CONCLUDING REMARKS

The natural convection problem was solved using a boundary-fitted coordinate method and the results compared with the experimental work of FLACK et alii(1979). The numerical results agreed well with the measurements when the average Nusselt number are compared.

The tentative of simulating the experimental work required the assumption of a temperature profile near the top corner of the cavity. The profile adopted resulted in local heat fluxes at the corner in considerable discrepancy with the experimental results. Despite the good agreement encountered in global basis, a better way to treat the heat transfer at the corner needs to be done in order to simulate more realistically the experiment. A step ahead to reach this goal would be to solve the conjugate problem involving conduction in the wall and convection in the fluid. This is presently being conducted by the authors.

NOMENCLATURE

x,y	cartesian coordinate system
ζ, η	general curvilinear coordinate system
J	Jacobian of the transformation

u,v	cartesian velocity components
T	temperature
P	pressure
α, β, γ	components of the metric tensor
C_1, C_2, C_3	transformed diffusivity for ϕ
t	time
ϕ	general scalar (u,v,T,...)
k_{eq}	equivalent conductivity, Eq.(5)
Gr	Grashof number, Eq.(3)
Ra	Rayleigh number (Gr Pr)
Nu	Nusselt number, Eq.(9)
q"	local heat flux; W/m ²
\bar{h}	average heat transfer coefficient
k_m	thermal conductivity evaluated at T_m
T_m	average temperature; $0.5(T_h + T_c)$
\bar{n}	normal
γ	angle in Fig. 2 and Eq.(3)

REFERENCE

FLACK, R.D., KONOPNICKI, T.T. and ROOKE, J.H. The measurement of natural convective heat transfer in triangular enclosures. ASME Journal of Heat Transfer, 101: 648-658, Nov. 1979.

FLACK, R.D. The experimental measurement of natural convection heat transfer in triangular enclosure heated or cooled from below. ASME Journal of Heat Transfer, 102: 770-772, 1980.

POULIKAKOS, D. and BEJAN, A. The fluid dynamics of an attic space. J. Fluid Mech., 131: 251-269, 1983.

MALISKA, C.R. and RAITHY, G.D. A method for computing three dimensional flows using non-orthogonal boundary-fitted co-ordinates, Int. J. Num. Meth. in Fluids, 4:519-537, 1984.

MALISKA, C.R. A solution method for three-dimensional parabolic fluid flow problems in nonorthogonal coordinates, Ph.D. thesis, Waterloo Univ., Ontario, Canada, 1981.

SCHNEIDER, G.E. and ZEDAN, M. A modified strongly implicit procedure for the numerical solution of field problems. Num. Heat Transfer, 4: 1-19, 1981.

ARPACI, V.S. Conduction heat transfer. Addison-wesley, Massachusetts, 1966.

DE VAHL DAVIS, G. and JONES, I.P. Natural convection in a square cavity: a comparison exercise. Int. J. Num. Meth. in Fluids, 3: 227-248, 1983.

TABLE I- \bar{E} , \bar{S} , and Γ expressions

ϕ	l	T	u	v
\bar{E}^ϕ	0	0	$P_{\xi}^y \eta - P_{\eta}^y \xi$	$P_{\eta}^x \xi - P_{\xi}^x \eta$
\bar{S}^ϕ	0	0	0	$[k_m C_B (T - \bar{T})] / J$
Γ^ϕ	0	$\alpha \alpha$	∂v	∂v

TABLE II- Geometric parameters

θ	γ	L(m)	W(m)	h(m)
60°	30°	0.0879	0.0879	0.0762
90°	45°	0.1078	0.1524	0.0762
120°	60°	0.1524	0.2637	0.0762

TABLE III- Nusselt number. Numerical x Experimental*

θ	Ra	0	4.91E6	6.38E6	3.96E6	5.21E6	2.75E6	3.55E6
60°	3.61		14.71	15.82				
				19.0				
90°	2.31				12.91	13.97		
					13.3	14.5		
120°	1.58						10.43	11.26
							10.0	11.0

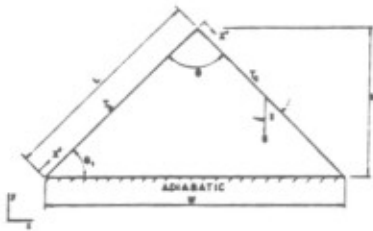


Fig. 1- Problem geometry

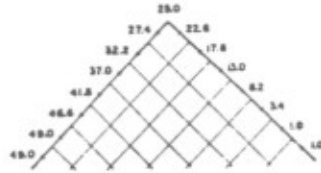


Fig. 5- Temperature profile at the tip

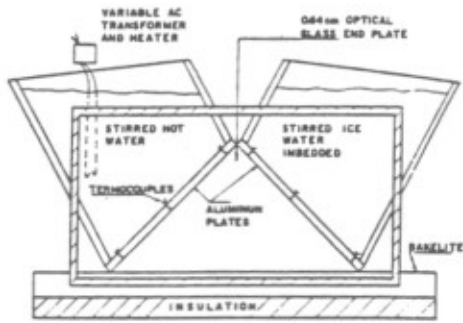


Fig. 2- Schematic of Flack's experiment

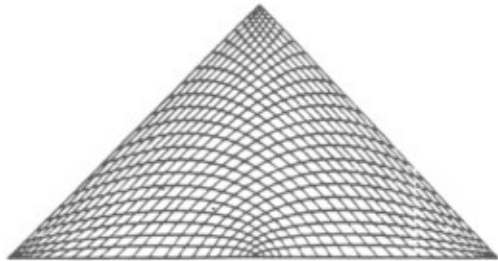


Fig. 3- Domain discretization; $\theta=90^\circ$

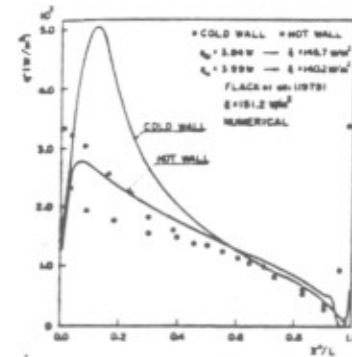


Fig. 4- Local heat fluxes

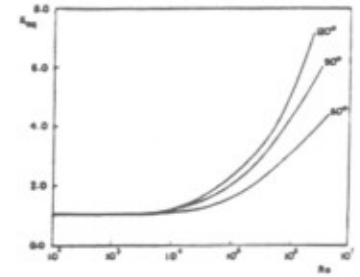


Fig. 6- Equivalent conductivity

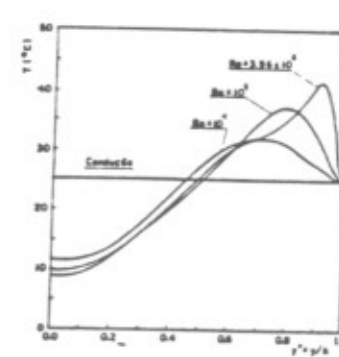


Fig. 7- Temperature profile; $\theta=90^\circ$

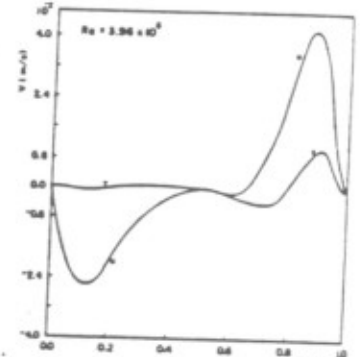


Fig. 8- Velocity profiles; $\theta=90^\circ$

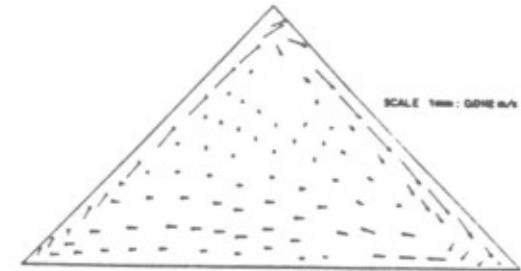


Fig. 9- Velocity vector plot; $\theta=90^\circ$, $Ra = 3.96 \times 10^6$